Atomic geometry and the probability distribution of self-assembled Cs nanowires at the InAs(110) surface

Maria Grazia Betti
Istituto Nazionale di Fisica della Materia–Dipartimento di Fisica, Università "La Sapienza," Piazzale Aldo Moro 2, I-00185 Roma, Italy

Valdis Corradini
Istituto Nazionale di Fisica della Materia–Dipartimento di Fisica, Università di Modena 1, Via G. Campi 213/A, I-41100 Modena, Italy

M. Sauvage-Simkin* and R. Pinchaux†
Laboratoire pour l'Utilisation du Rayonnement Electromagnétique (LURE), Bat. 209D, Université Paris-Sud, F-91405 Orsay, France
(Received 28 September 2001; revised manuscript received 13 December 2001; published 30 August 2002)

Cesium adsorbs on the InAs(110) surface in the form of long chains extending for several hundreds angstroms along the $[1\bar{1}0]$ direction, leading to a $(2\times n)$ periodicity, with n depending on the mean distance between the alkali chains. We have investigated the evolution of the $(2\times n)$ superstructure as a function of coverage and the statistical distribution of the Cs chains by means of grazing-incidence x-ray diffraction and low-energy electron diffraction. The atomic geometry has been fully determined: each Cs chain is constituted by two Cs adatoms with different adsorption sites. The minimum Cs-Cs distance within the chain is 6.9 Å, much larger than the Cs-Cs bond length in bcc bulk metallic Cs.

DOI: 10.1103/PhysRevB.66.085335 PACS number(s): 68.43.Hn, 61.10.−i, 68.65.−k

I. INTRODUCTION

The design of nanoscale devices requires the fabrication of nanostructures with a well-controlled architecture at the atomic scale. Two avenues are presently being exploited in which nanostructures are constructed using surface techniques. The first approach involves manipulation of individual atoms or molecules with a scanning tunneling microscope (STM) tip, while an alternate method is to use templates to pattern the overlayer growth. Self-organization and self-assembly on a solid surface is a promising alternative for growing uniform nanostructures with regular size and spacing.[1–5] Alkali metals adsorbed on suitable substrates are appealing model systems to investigate the self-assembling of nanowires. As a prototype of these systems, Cs adatoms deposited on III-V(110) surfaces self-assemble, forming chains extending for several hundreds angstroms.[5–9]

Scanning tunneling microscopy studies have yielded considerable insight into the local structure of alkali nanowires, showing the local atomic topography for Cs deposited on GaAs(110), InSb(110), and InAs(110) substrates.[5–9] The Cs adatoms form regular one-dimensional (1D) zigzag chains oriented along the $[1\bar{1}0]$ direction even at a very low coverage. The distribution of the Cs chain distances is always far removed from the exponential distribution typical of a random process. The chains repel each other in the [001] direction even when their mutual distance is larger than 50 Å.[9] Generally, alkali atoms adsorbed on metallic substrates spread out owing to the long-range repulsion induced by strong dipolar interactions,[10,11] while they occupy 1D channels when deposited on the (110) surfaces of noble metals in the presence of missing-row reconstructed surfaces.[12] Total energy calculations for alkali deposited on III-V(110) surfaces show a topology of the energy surface with a high anisotropy perpendicular to the $[1\bar{1}0]$ direction and a small barrier parallel to the chain direction, favoring a migration of the alkali adatoms in the channels between the substrate chains.[10,13]

Despite a great research effort devoted to alkali nanowires, several questions are still open regarding the atomic geometry and its specific interrelationship with the electronic properties. Cesium chains self-assembled on III-V(110) surfaces are insulating in the whole coverage range.[14,15] Several theoretical approaches have been applied to study the electronic structure of alkali metals on III-V(110) surfaces. A simple atomic geometry is generally assumed, with a single alkali atom adsorption site close to the substrate cation.[13,16–18] The nonmetallic behavior is justified as an example of a Mott insulator.[13,14,18] Recently, *ab initio* density functional calculations of Cs chains formation on the InAs(110) surface have been reported, showing a insulating (2×2) superstructure: the minimum energy configuration was obtained for two distinct and inequivalent adsorption sites,[19,20] confirming core-level photoemission results.[21–24] The long-range ordering of the alkali nanowires, the probability distribution of the chains, and a precise determination of the atomic geometry are required for a deeper understanding of this system.[25]

The aim of this paper is to provide the atomic geometry of the Cs chains and the mesoscopic properties (i.e., chain probability distribution) of self-assembled nanowires deposited on the InAs(110) surface by surface x-ray diffraction. Cesium atoms, adsorbed on an InAs(110) surface, form chains characterized by two inequivalent Cs adsorption sites and a slight modification of the substrate topmost layer, preserving the topology of the relaxed III-V(110) surface. The alkali chain self-assembling can be followed by analyzing the diffuse scattering in the diffraction data on the basis of a probability distribution of the pseudo $(2\times n)$ reconstructions using the phase-matrix method.[26,27] The Cs chain probability distribution is far from a random process and in agreement with STM observations.[9] The study of the statistical distribu-

tion of the Cs nanowires via the surface diffraction technique can be considered a model case to investigate the mesoscopic properties of long-range-ordered nanostructures and to determine the driving forces of self-assembly and self-organization on suitable surface templates.

II. EXPERIMENT

The InAs(110) single crystal was a polished wafer provided by Wafer Technologies. The clean surface has been obtained after subsequent cycles of sputtering and annealing. Cesium was evaporated from well-outgassed resistively heated dispensers, keeping the base pressure within 2×10^{-10} mbar during deposition. In the following the Cs coverage $\Theta_s=1$ corresponds to the saturation coverage as determined by Auger peak intensity.

The GIXD experiment was carried out at the wiggler beamline DW12 of the DCI storage ring at the LURE synchrotron radiation facility, in an ultrahigh-vacuum (UHV) chamber equipped with a six-circle diffractometer, coupled to sample preparation chambers containing all the ancillary equipment for crystal preparation and characterization. The grazing-incidence x-ray diffraction data were recorded with a focused radiation of 15 keV at the critical incidence angle for total reflection on indium arsenide ($\alpha_c=2\times10^{-3}$ rad at $\lambda=0.83$ Å). The base pressure in the chambers was kept below 1×10^{-10} mbar (1×10^{-8} Pa).

The InAs(110) (2×2) surface reciprocal unit cell is hereafter labeled by the h and k indexes along the $[1\bar{1}0]$ and [001] directions, respectively. Integer-order diffraction data have been first collected in the standard angular scan mode, both at in-plane Bragg positions and along the integer rods normal to the surface. This procedure allowed a first assignment of the atomic positions in the surface unit cell. For the pseudo $(2\times n)$ phase, with n depending on the chain distance, a continuous intensity distribution was measured in the direction perpendicular to the chains.

III. RESULTS

A. $(2\times n)$ periodicity: LEED and diffuse scattering

We have followed the symmetry and periodicity evolution of the self-assembled Cs chains as a function of alkali coverage, looking at the evolution of the low-energy electron diffraction (LEED) patterns. In Fig. 1 we report LEED patterns for the clean InAs(110) surface and at 35%, 45%, and 50% of Cs saturation coverage θ_s. Electron diffraction data show a pseudo-long-range-ordered $(2\times n)$ symmetry, with broad extra spots due to the ordering of the Cs chains. The position of the extra spots strongly depends on the Cs coverage, as it shifts from the integer-order spots towards the midpoint of the reciprocal cell side in the [001] direction, upon increasing Cs exposure. The evolution of the $(2\times n)$ superstructure can be related to the packing of the Cs chains as a function of Cs coverage. The intensity distribution of the diffuse scattering in the direction perpendicular to the chains, measured by grazing-incidence x-ray diffraction, is expected to present an analogous behavior. The diffuse x-ray scattering intensity evolution along the k direction at fixed h value

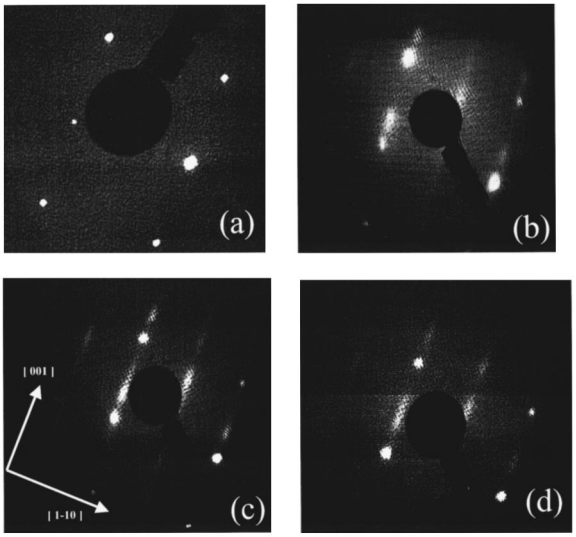

FIG. 1. Low-energy electron diffraction patterns for the InAs(110) clean surface (a), at 35% (b), 45% (c), and 50% (d) of the saturation coverage θ_s. The stripes indicate a $\times2$ periodicity along the $[1\bar{1}0]$ direction (present in all patterns even at low Cs coverages) and a $\times n$ superstructure along the direction [001] perpendicular to the chains with n decreasing as a function of Cs chain density.

is shown in Fig. 2(a), for different Cs exposures (30%, 50%, and 60% of the saturation coverage). It confirms the $(2\times n)$ periodicity, it shows maxima corresponding to the position of the extra spots in the LEED patterns and the maxima shift towards half order k values at increasing coverage. The evolution of the LEED pattern and of the diffuse x-ray scattering can be explained following the Cs chain

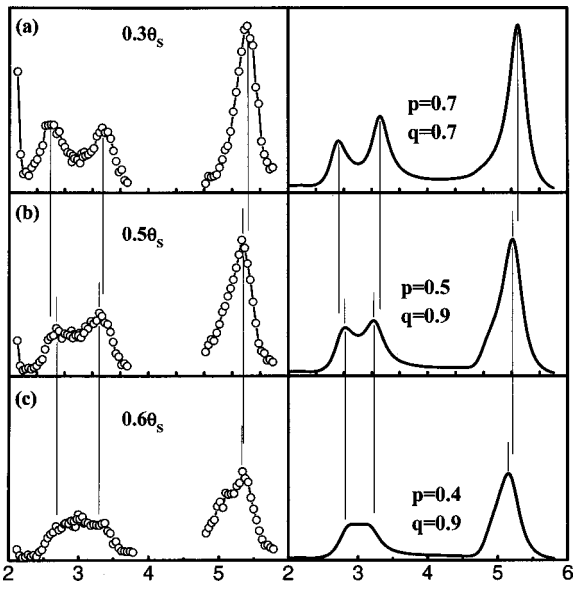

FIG. 2. Diffuse scattering as measured by means Grazing-incidence x-ray diffraction collected along the k reciprocal unit direction at $h=0$. Left panel: experimental data at 30% (a), 50% (b), and 60% (c) of saturation coverage θ_s. Right panel: diffuse scattering simulations using the diffuse matrix method for the corresponding Cs density at different p and q probabilities.

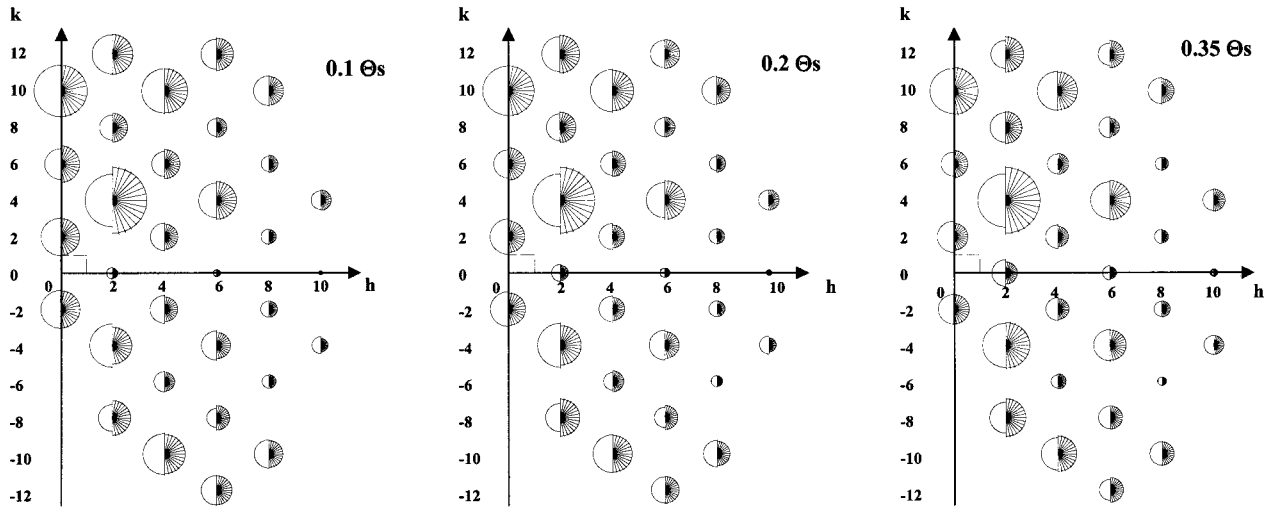

FIG. 3. Comparison between experimental (shaded semicircle) and best fit calculated (open semicircles) in-plane structure factors at three different Cs coverages 10% (a), 20%(b), and 35% (c). The radius of the circle is proportional to the structural factor.

packing, as deduced from STM.[9] The STM topography shows regular one-dimensional zigzag chains in the [110] direction, constituted by couples of Cs atoms with a mutual couple-couple distance of about 8 Å, corresponding to twice the surface cell lattice vector in the $[1\bar{1}0]$ direction. The parallel Cs wires are spaced by multiples of the surface lattice constant along the [001] direction. From the diffraction data, at low coverage the $(2\times n)$ superstructure has high n values, corresponding to chain-chain distances in the range 50–100 Å. At higher coverage n decreases, as the chain packing increases, thus confirming a minimum chain-chain distance of 12 or 18 Å, as observed by STM (2 or 3 times the surface unit cell). A simulation of the diffuse scattering as a function of p and q probabilities is reported in Fig. 2(b), and it will be discussed in the last section. The probability of the Cs/InAs(110)-(2×2) unit cell (named A block) to be followed by a clean relaxed InAs(110) double unit cell (named B block) is labeled p, and q is the probability of the B block to be followed by the A block. The A block introduced in the simulation is the Cs/InAs(110)-(2×2) atomic geometry, as deduced from the GIXD data reported in the following section.

B. Structural model

A complete set of 32 nonequivalent in-plane (hk) beams has been collected at $l=0.1$ reciprocal space units. The evolution of (hk) rods has been measured as a function of l up to a perpendicular momentum transfer of about 4 Å^{-1}. The diffuse scattering due to the $(2\times n)$ periodicity has been recorded in the k direction, as previously reported in Fig. 2(a). The diffraction data have been collected at different Cs exposures (10%, 20%, 35%, and 50% of saturation coverage θ_s) in order to follow the evolution of the chains structure as a function of the self-assembly.

The structure factors have been derived by applying the proper correcting factor to the integrated measured intensities, taking into account the variation of the Lorentz and polarization factors and of the sample active area. The sets of the in-plane reflections and of the rod scans have been compared with a structural model through a least-squares fitting minimization on the variable parameters allowing in-plane and out-of-plane displacements. We have determined the atomic geometry of the Cs chains and of the underlying InAs(110) substrate at different Cs coverages using a (2×2) cell with ten independent atoms. The chain density on the surface has been taken into account, introducing a different percentage of clean InAs(110) relaxed surface at different Cs chain coverages. The best fitting procedure is obtained imposing the same atomic coordinates for the whole set of data at different Cs exposures, only changing the occupancy of Cs chains: OC=0.12 for 10% of θ_s, OC=0.3 for 20%, OC=0.5 for 35%, and OC=0.75 for 50%. A set of structural models has been tried to fit the in-plane structure factors, considering the constraints derived from complementary experimental achievements.[9,10] In fact, previous experimental results[5] and theoretical investigations[13] suggested that alkali adsorption on III-V(110) surfaces would occur by a preferential adsorption site close to the cation dangling bonds. However, an atomic geometry of the chain with equivalent Cs sites can be excluded, since the Cs core-level photoemission spectra clearly show two different components with an energy shift of about 0.65 eV.[22] Moreover, an atomic geometry with only one Cs adsorption site does not account for the attractive interaction between Cs adatoms leading to long chains and appears to be more consistent with the formation of a layer assembled via a random process. A further model, deduced from recent theoretical calculations, has proposed a stable atomic geometry of Cs on InAs(110) with a (2×2) periodicity, where couples of Cs adatoms 6.57 Å distant are forming long stable chains.

The experimental and best-fit calculated structure factors are reported in Fig. 3 for the in-plane data at different Cs coverages $\theta=0.10\theta_s$ ($\chi^2=1.4$), $\theta=0.20\theta_s$ ($\chi^2=1$), and $\theta=0.35\theta_s$ ($\chi^2=1$) and in Fig. 4 for the rod scan at $\theta=0.35\theta_s$. The main difference in the structure factors is the symmetry breaking with respect to the $k=0$ plane and an

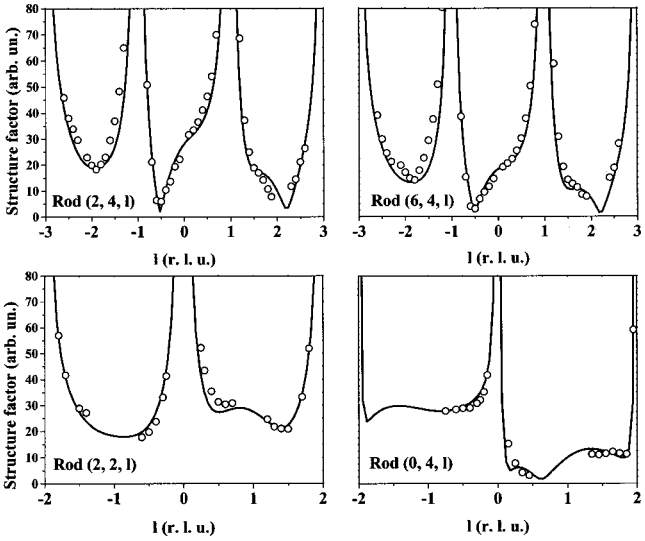

FIG. 4. Experimental (dots) and best-fit calculated (solid line) structure factors in the rod scans.

increasing intensity of the diffracted peaks with the $k=0$ and $h=2,6,10$ along the $[1\underline{1}0]$ reciprocal bulk direction on increasing the Cs chain density (Fig. 3). Information about the atomic displacements in the direction perpendicular to the surface can be obtained by fitting the set of rod scans reported in Fig. 4.

A full structure determination has been achieved, and the resulting atomic geometry of the Cs chains for the (2×2) superstructure is shown in Fig. 5. The proposed geometry confirms the presence of two nonequivalent Cs adsorption sites (Cs_1 and Cs_2). In Table I we report the Cs_1 and Cs_2 atomic positions in the (2×2) surface unit cell and the atomic position of the underlying InAs topmost layer. In Table II the Cs_1-Cs_2 distance and the bond lengths of the Cs adatoms with the In near neighbors are compared with the distances predicted by *ab initio* total energy calculations.[19,20] The atomic positions projected on the (110) surface plane can be determined with a high degree of accuracy for the whole set of data, while the corresponding out-of-plane positions have a higher uncertainty as reported in Table I. The Cs_1 adatom is positioned along the In_2 dangling bond, the Cs_2 adatom between the In_3 and As_3 atoms. Although the Cs adsorption to the In dangling bonds seems energetically favorable, the Cs_1-Cs_2 distance in the chain is 6.9 Å, lower than the Cs-Cs distance with equivalent adsorption sites on the cation surface atoms (7.5 Å). The Cs-Cs distance is about 50% larger than the bond length in bcc bulk metallic Cs (5.24 Å). This scenario is in agreement with the topography deduced from the STM images,[9] the theoretical predictions of a Cs-Cs distance of 6.57 Å,[20] and with the core-level photoemission results.[21] From the STM images we can also infer more complex structures like broad Cs chains at higher coverage. In the present analysis, this structural configuration and the presence of a further clustering have not been taken into account. They probably influence the structural factors at higher coverage (more than 50% of saturation) where a lower reliability factor has been obtained fitting the GIXD data.

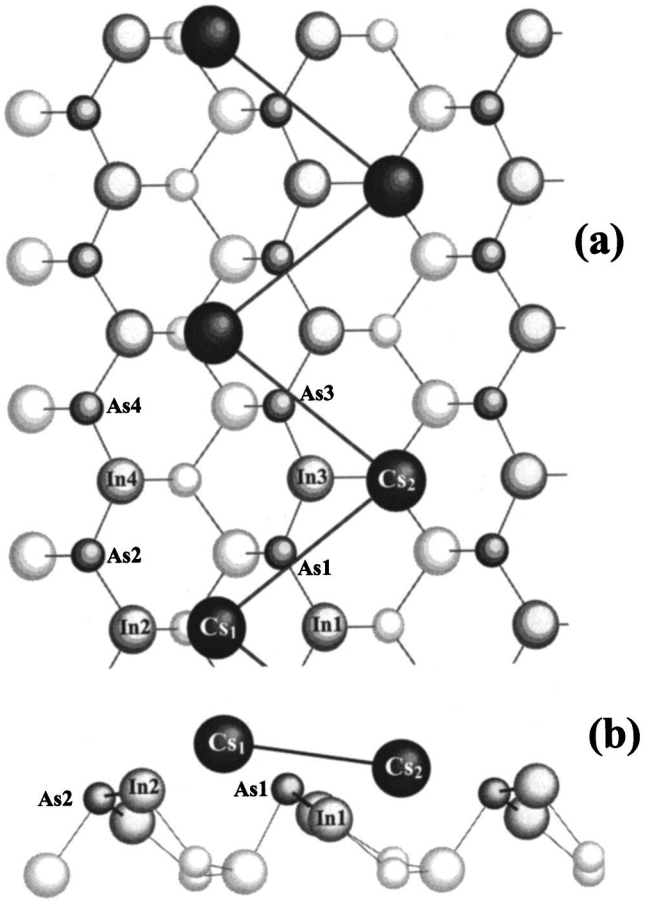

FIG. 5. Top view of the (110) plane considering the atomic displacements deduced by the best-fitting procedure for the (2×2) Cs/InAs(110) phase. The Cs adatoms are labeled showing inequivalent adsorption sites (Cs_1 and Cs_2) along the chain; the topmost and second InAs layers are reported. (b) Side view of the Cs adatoms and InAs underlying layers.

The surface geometry of the topmost InAs(110) layer is locally modified, while the relaxed configuration of the In and As atoms not bounded to the Cs chains is preserved (see Fig. 5). The In_2 atom close to the Cs_1 site moves outwards, reaching a position close to the ideal bulk site. The In_2-Cs_1 distance is 2.87 Å. The In_3-Cs_2 distance is larger (2.92 Å) and an electronic-level rehybridization on the underlying As_3 and In_3 atoms is observed. The In_3 is downward displaced with respect to the relaxed surface position, as shown in Fig. 5. The nonequivalent adsorption sites, a prevalent charge transfer between the Cs_1 and In_2 atoms, and a Cs_1-Cs_2 interaction mediated by the substrate are at the origin of the attractive interaction between the adjacent coupled Cs adatoms within each self-assembled nanowire. A deep understanding of the driving forces leading to the insulating nature can be accomplished with an accurate theoretical study of the chain electronic properties considering the actual geometry. The only band structure calculation, performed with a similar atomic geometry, presents a state in the semiconductor energy gap due the complete filling of the In dangling bond. A symmetric geometry with equivalent Cs sites is unfavorable and the band structure presents two degenerate semioccupied

TABLE I. Atomic coordinates derived from the best fit of the x-ray diffraction data and referred to the 2×2 unit cell. ($a^1=8.567$ Å, $b^1=12.116$ Å, $c^1=4.284$ Å.) See Fig. 4 for identification of atom labels.

	x	y	z
Cs_1	0.00 ± 0.01	0.30 ± 0.01	0.94 ± 0.05
Cs_2	0.49 ± 0.01	0.85 ± 0.01	0.75 ± 0.05
In	0.000 ± 0.005	0.032 ± 0.005	0.39 ± 0.02
As_1	0.250 ± 0.005	0.140 ± 0.005	0.61 ± 0.02
In_2	0.000 ± 0.005	0.506 ± 0.005	0.61 ± 0.02
As_2	0.250 ± 0.005	0.615 ± 0.005	0.56 ± 0.02
In_3	0.500 ± 0.005	0.062 ± 0.005	0.43 ± 0.02
As_3	0.750 ± 0.005	0.140 ± 0.005	0.61 ± 0.02
In_4	0.500 ± 0.005	0.532 ± 0.005	0.39 ± 0.02
As_4	0.750 ± 0.005	0.615 ± 0.005	0.56 ± 0.02

(metalliclike) (Ref. 20) bands. Preliminary angular-resolved photoemission experiments show a Cs-induced electronic band which is dispersive in the $[1\bar{1}0]$ direction, associated with the chain and well below the Fermi energy, confirming the absence of a density of states at the Fermi energy in the whole surface Brillouin zone.

C. Analysis of the diffuse scattering: Model for the $(2\times n)$ phase

The occurrence of a pseudo $(2\times n)$ phase has been clearly observed in the LEED patterns and attested to by measuring the diffuse scattering in the grazing-incidence x-ray experiment as reported in Figs. 1 and 2. The analysis of the diffuse scattering can give further confirmation of the atomic geometry of the Cs chains and useful information on the mesoscopic properties of the self-assembling process (i.e., probability distribution of the chain-chain distance).

The evolution of the $(2\times n)$ superstructure can be related to the distances between the Cs chains as a function of Cs coverage, in agreement with the statistical distribution deduced by scanning tunneling microscopy topography. The diffuse scattering distribution can be derived by a theoretical simulation considering a sequence of *A* and *B* blocks, where the *A* block represents the structural model of the Cs/InAs(110)-(2×2) unit cell and the *B* block represents the (1×2) clean relaxed InAs(110) double unit cell. A schematic view of this sequence is reported in the top panel of Fig. 6. The simulation of the diffuse scattering distribution, calculated with the phase-matrix method, is a function of two probabilities $p(BA)$, which is the probability of the *A* block to be followed by the *B* block, and $q(AB)$, which is the probability of the *B* block to be followed by the *A* block.

TABLE II. Bond distances in Å of Cs and the substrate atoms as obtained from the best fit of the GIXD data. In Ref. 19 the inequivalent Cs adsorption sites are along In2 and As2 dangling bonds, respectively, while in Ref. 20 are along the In2 and In3 dangling bonds.

	$d_{Cs1\text{-}Cs2}$ (Å)	$d_{Cs1\text{-}In2}$ (Å)	$d_{Cs2\text{-}In3}$ (Å)	$d_{Cs2\text{-}As2}$ (Å)
GIXD	6.9 ± 0.2	2.87 ± 0.1	2.92 ± 0.1	
Theory (Ref. 19)	6.99	3.74		3.73
(Ref. 20)	6.57			

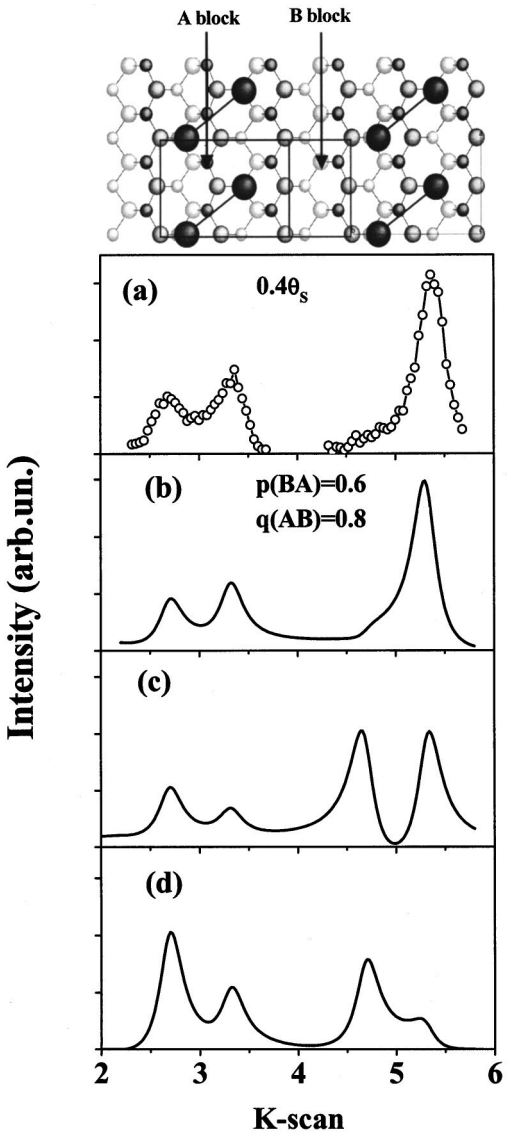

FIG. 6. Upper panel: InAs(110) plane with Cs adatoms in the reconstructed (2×2) unit cell (*A* block) alternate with the clean InAs surface with a (1×2) unit cell (*B* block). The sequence *ABAB* with a (2×3) periodicity is simulated with $p=1$ and $q=1$, while a sequence *AAA* has a $p=0$ and $q=1$ probability. (a) Diffuse scattering experimental data at 0.4 Θ_S compared with different structural models. (b) Geometry obtained from the best fit of present GIXD data. (c) Single Cs adsorption site as reported in Refs. 5 and 13. (d) Geometry deduced from theoretical calculations reported in Ref. 10.

In Fig. 6 we compare the diffuse scattering experimental data (a) at 40% of saturation coverage and the theoretical simulations for different structural models proposed: (b) the model deduced from the best fit of the GIXD experimental results reported in Fig. 5, (c) the atomic structure with

TABLE III. Probability distribution (p, q) of the Cs chains as a function of Cs exposure θ. The Cs chain distance is reported as a multiple of the lattice vector a_0 (6.058 Å) of the (1×1) InAs(110) substrate unit cell. The percentage of Cs distance, the chain average distance L_{ave}, and the chain density (occupancy OC) are derived from the phase matrix simulation. The results are compared with the statistical distribution deduced from the STM topography.

Cs coverage	p	q	Cs chain distance $2a_0$ (12 Å)	$3a_0$ (18 Å)	$4a_0$ (24 Å)	L_{ave} (Å)	OC
$0.3\theta_s$	0.7	0.7	30%	49%	15%	18.2	0.55
$0.4\theta_s$	0.6	0.8	40%	48%	10%	16.7	0.75
$0.5\theta_s$	0.5	0.9	50%	45%	5%	15.5	0.78
$0.6\theta_s$	0.4	0.9	60%	36%	4%	14.8	0.82
$0.48\theta_s$ STM (Ref. 9)			57%	40%	3%	15	

equivalent Cs adsorption sites bonded to the In cations, and (d) the theoretical model deduced from the first-principles calculations reported in Ref. 21. Our model (b) is in very good agreement with the whole set of diffuse scattering experimental data as can be observed also for the different occupancies of the Cs chains reported in Fig. 2(b).

From the probability parameters (p, q) derived from the phase-matrix simulation, we can deduce the chain density, the average chain distance (L_{ave}), and the occupancy of the Cs chains for the $(2\times n)$ incommensurate phases, as displayed in Table III. At $0.3\theta_s$, with $p=0.7$ and $q=0.7$, we derive 30% of probability to have Cs chains distant 12 Å, 49% distant by 18 Å, and 15% distant by 24 Å, with an average chain distance L_{ave} of about 18.2 Å. At this coverage, 55% of the InAs(110) surface is covered with Cs chains. When increasing the Cs chains density, the average chain distance saturates at a value of about 15 Å, with 60% of Cs chains distant twice the InAs(110) substrate unit cell and 36% distant by three times a_0. The Cs-chain distance distribution is in very good agreement with the STM statistical investigations, reported in Ref. 9, as shown in Table III. In the last column of Table III the ratio of Cs-chain-filled surface obtained by the simulation of the diffuse scattering distribution is reported; the behavior is in really good agreement with the occupancy parameters previously obtained by the fitting procedure of the in-plane diffracted intensities.

IV. CONCLUSIONS

A comparative study of the atomic geometry and the mesoscopic properties of the Cs chains by means of diffraction techniques is presented. The alkali chains are constituted by adjacent couples of Cs adatoms with two adsorption sites. The analysis of the diffuse scattering along the k reciprocal axis gives useful information to determine the probability distribution of the nanowires at different Cs coverages and confirms the structural model proposed. The mesoscopic properties of the self-assembled chains show a probability distribution of the chain distances far removed from the exponential distribution of a random nucleation process. A full determination of the electronic band structure of the Cs chains is clearly needed in order to disentangle the influences of correlation effects and/or atomic geometry on the insulating character of alkali chains deposited on III-V(110) surfaces.

ACKNOWLEDGMENTS

We thank Yves Garreau for the experimental support and fruitful discussions. We thank Oscar Moze for a critical reading of the manuscript. The European Union, under the Large Installation Project, is warmly thanked for the support to work at LURE. This research is financed by the Ministero per l'Università e per la Ricerca Scientifica e Tecnologica and by the Consiglio Nazionale delle Ricerche (CNR).

*Also at Laboratoire de Minéralogie-Cristallographie, 4 Place Jussieu, 75252 Paris-Cedex 05, France

†Also at Université Pierre et Marie Curie, 4 Place Jussieu, 75252 Paris-Cedex 05, France

[1] Feng Liu, J. Tersoff, and M. G. Lagally, Phys. Rev. Lett. **80**, 1268 (1998).

[2] V. A. Shchukin and D. Bimberg, Rev. Mod. Phys. **71**, 1125 (1999).

[3] K. N. Altmann, J. N. Crain, A. Kirakosian, J.-L. Lin, D. Y. Petrovykh, F. J. Himpsel, and R. Losio, Phys. Rev. B **64**, 035406 (2001).

[4] J.-L. Lin, D. Y. Petrovykh, A. Kirakosian, H. Rauscher, F. J. Himpsel, and P. A. Dowben, Appl. Phys. Lett. **78**, 829 (2001).

[5] L. J. Whitman, Joseph A. Stroscio, R. A. Dragoset, and R. J. Celotta, Phys. Rev. Lett. **66**, 1338 (1991).

[6] P. N. First, R. A. Dragoset, Joseph A. Stroscio, R. J. Celotta, and R. M. Feenstra, J. Vac. Sci. Technol. A **7**, 2868 (1989).

[7] L. J. Whitman, Joseph A. Stroscio, R. A. Dragoset, and R. J. Celotta, Phys. Rev. B **44**, 5951 (1991).

[8] L. J. Whitman, Joseph A. Stroscio, R. A. Dragoset, and R. J. Celotta, J. Vac. Sci. Technol. B **9**, 770 (1991).

[9] S. Modesti, A. Falasca, M. Polentarutti, Maria Grazia Betti, V. De Renzi, and Carlo Mariani, Surf. Sci. **447**, 133 (2000).

[10] For a review, see *Physics and Chemistry of Alkali Metal Adsorption*, edited by H. P. Bonzel, A. M. Bradshaw, and G. Ertl (Elsevier, Amsterdam, 1989).

[11] R. Schuster, J. V. Barth, and G. Ertl, Surf. Sci. **247**, L229 (1991).

[12] S. Chandravarkar and R. D. Diehl, Phys. Rev. B **38**, 12 112

(1988).
[13] F. Bechstedt and M. Scheffler, Surf. Sci. Rep. **18**, 145 (1993), and references therein.
[14] T. Maeda Wong, D. Haskett, N. J. Di Nardo, and E. W. Plummer, Surf. Sci. **208**, L1 (1989).
[15] J. Ortega and F. Flores, Phys. Rev. Lett. **63**, 2500 (1989); C. Y. Fong, L. H. Yang, and Inder P. Batra, Phys. Rev. B **40**, 6120 (1989); J. Ortega, R. Pérez, F. J. García-Vidal, and F. Flores, Surf. Sci. **56–58**, 264 (1992), B. Croset and C. de Beauvais, *ibid.* **409**, 403 (1998).
[16] X. W. Wang and Changfeng Chen, Phys. Rev. B **54**, 13 436 (1996); Changfeng Chen and W. W. Wang, J. Phys.: Condens. Matter **10**, 731 (1998).
[17] Jörk Hebenstreit, Martina Heinemann, and Matthias Scheffler, Phys. Rev. Lett. **67**, 1031 (1991); Jörk Hebenstreit and Matthias Scheffler, Phys. Rev. B **92**, 10 134 (1992).
[18] Oleg Pankratov and Matthias Scheffler, Phys. Rev. Lett. **71**, 2797 (1993); Surf. Sci. **287/288**, 584 (1993).
[19] A. Calzolari, C. A. Pignedoli, R. Di Felice, C. M. Bertoni, and A. Catellani, Surf. Sci. **454–456**, 207 (2000).
[20] A. Calzolari, C. A. Pignedoli, R. Di Felice, and C. M. Bertoni, Surf. Sci. **491**, 265 (2001).
[21] Maria Grazia Betti, V. Corradini, S. Gardonio, G. Bertoni, C. Mariani, L. Gavioli, R. Belkou, and A. Taleb-Ibrahimi, Surf. Sci. **477**, 35 (2001).
[22] Maria Grazia Betti, S. Morucci, L. Gavioli, R. Belkou, and A. Taleb-Ibrahimi (unpublished).
[23] G. Faraci, A. R. Pennisi, F. Gozzo, S. La Rosa, and G. Margaritondo, Phys. Rev. B **53**, 3987 (1996).
[24] K. M. Schirm, P. Soukiassian, P. S. Mangat, and L. Soonckindt, Phys. Rev. B **49**, 5490 (1994).
[25] T. Maeda Wong, N. J. DiNardo, D. Heskett, and E. W. Plummer, Phys. Rev. B **41**, 12 342 (1990); P. S. Mangat and P. Soukiassian, Phys. Rev. B **52**, 12 020 (1995).
[26] B. Croset and C. de Beauvais, Surf. Sci. **409**, 403 (1998).
[27] C. S. Lent and P. I. Cohen, Surf. Sci. **139**, 121 (1984).